Analytical Study of Reusable Flight-Weight Cryogenic Propellant Tank Designs

Allan H. Taylor*
NASA Langley Research Center, Hampton, Virginia
Jeffrey A. Cerro†
PRC Kentron Inc., Hampton, Virginia
and
L. Robert Jackson‡
NASA Langley Research Center, Hampton, Virginia

A pacing technology for fully reusable space launch vehicles and hypersonic flight in the atmosphere is the development of reusable, flight-weight, cryogenic propellant tanks. Results of an analytical study of three cryogenic tank structural concepts, each suspended within a carbon-carbon aeroshell structure, are presented. The first tank concept is a honeycomb-core sandwich structure with an evacuated core providing the cryogenic insulation. The second tank concept is an integrally stiffened skin structure using a low-density, closed-cell, cryogenic foam insulation, and the third is an unstiffened skin structure using the same foam insulation. The effect of various design parameters on the tank weight was evaluated. The tanks were sized primarily by ullage pressure, hydrostatic pressure, and aeroinertial loads. However, compatibility with the propellants, fracture mechanics, thermal stress, minimum gage constraints, and temperature limitations was also considered. Design curves are presented that show the effect of variations in several of the design parameters on tank wall thickness. These design curves are used as analytical tools to size reusable, flight-weight cryogenic tanks for a baseline space launch vehicle. The results indicate that a pressure-stabilized, unstiffened-skin, aluminum tank with a 400°F cryogenic insulation is the least weight for most design conditions.

Nomenclature

ACC = advanced carbon-carbon
E = modulus of elasticity, psi
g = acceleration due to gravity, ft/s^2
K_I = stress intensity factor
M = Mach number
N = load intensity, lb/in.
R = radius, in.
S = stress, psi
t = equivalent thickness, in.
θ = tank segment angle, deg

Subscripts

x,y,z = axial, lateral, and vertical directions, respectively

Introduction

FROM the advent of rocket-propelled launch vehicles, cryogenic propellants have been employed due to their high specific impulse and resulting propulsion efficiency. While space launch vehicles have matured from relatively small, simple, expendable systems to large, complex, generally reusable systems over the last 40 years, the cryogenic tank designs have remained basically unchanged. Current cryogenic tanks are cylindrical structures, either an integrally stiffened, aluminum skin structure (V-2, Saturn, Shuttle external tank) or a pressure-stabilized, unstiffened, stainless-steel skin structure (Atlas, Centaur). These tank structures have been expendable, which increases the cost of each launch. Currently no aircraft use cryogenic fuels; however, cryogenically fueled aircraft have been studied for over 30 years.[1]

Fully reusable cryogenic tanks are required to meet a stringent set of design requirements and to maintain leak-free containment for the vehicle's design life. An equally important consideration is the cryogenic insulation system used to prevent condensation of gases on the tank and excessive cryogen boiloff. The advent of new materials, manufacturing processes, and analytical techniques allow the design engineer more freedom in selecting efficient structural concepts to meet these requirements.

This paper describes the results of an analytical study of three cryogenic tank structural concepts applied to a specific baseline vehicle. The first concept is a honeycomb-core sandwich structure with an evacuated honeycomb core providing the cryogenic insulation. The second and third concepts use integrally stiffened and unstiffened skin structures, respectively, with a low-density, closed-cell, foam cryogenic insulation. These concepts are evaluated for the least unit weight required to satisfy the structural design criteria.

Baseline Vehicle Description

For this study, an advanced space transportation system is used as the baseline vehicle. The structural arrangement of this vehicle (Fig. 1) consists of integral cryogenic tanks and a thrust structure encapsulated within a separate wing-fuselage structure (aeroshell) supported within the fuselage structure by aft trunnion and forward hinge supports. The aeroshell is a hot structure with internal blanket insulation that maintains the temperature of the tank structure below its maximum service temperature when the fuselage is subjected to aerodynamic heating. The baseline vehicle is described more fully in Refs. 2 and 3.

Wall Construction Details

Sections through fuselage and tank walls are shown in Fig. 2. The aeroshell wall with the packaged fibrous insulation is common for all tank concepts. However, the amount of

Received April 12, 1984; presented as Paper 84-0865 at the AIAA/ASME/ASCE/AHS 25th Structures Structural Dynamics and Materials Conference, Palm Springs, CA, May 14-16, 1984; revision received July 25, 1985.

*Aerospace Engineer. Associate Fellow AIAA.
†Senior Structures Engineer, Aerospace Technologies Division. Member AIAA.
‡Aerospace Engineer.

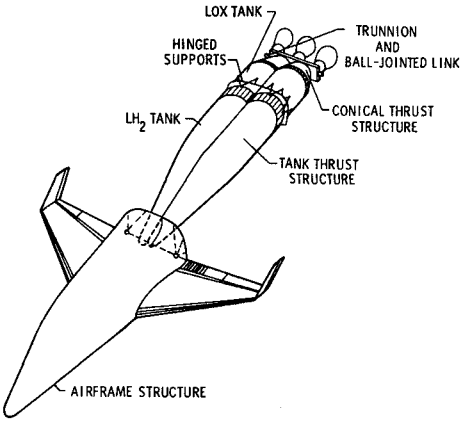

Fig. 1 Baseline vehicle.

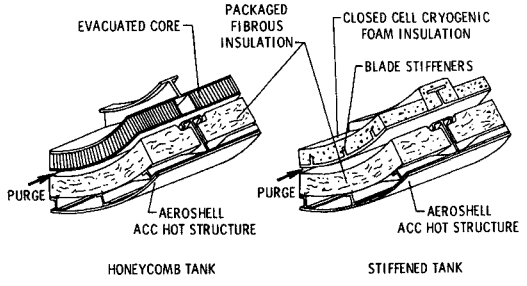

Fig. 2 Wall construction details for two cryogenic tank concepts.

fibrous insulation required varies depending on the temperature limit of the exterior tank surface. In all concepts, the tank walls are welded to provide leak-free containment of the cryogens. As shown, the honeycomb-core sandwich concept uses an evaluated titanium-alloy core to provide the cryogenic insulation. In this concept, the core thickness is varied to provide the required insulation. For the integrally stiffened and unstiffened tanks, a closed-cell foam provides the cryogenic insulation and the foam thickness is varied to meet the insulation requirements. In Fig. 2, the foam is shown on the interior of the tank wall, which is acceptable for liquid hydrogen (LH_2). However, the organic foams are sensitive to liquid oxygen (LOX)[4]; i.e., they burn in the presence of LOX with very little ignition energy. Therefore, for LOX tanks, the foam insulation is required to be on the tank wall exterior. The foam thickness was evaluated on the exterior surface of the LOX and LH_2 tanks and on the interior surface of the LH_2 tank. The right-hand side of Fig. 2 shows an integrally stiffened tank skin. For an unstiffened skin, the blade stiffeners are removed.

The cryogenic tanks are used as a reference point design for the baseline vehicle in this analysis. Alternate tank wall designs are assessed, and data are presented on the effect of changing the design variables for a range of tank sizes.

Design Criteria

Specific design criteria are required for each vehicle concept. However, it is beyond the scope of this paper to address all of the criteria, such as slosh loads, asymmetric pressure loads, and specific point loads, that would be required in the detailed design of a tank. For conceptual or preliminary design studies a subjective list of the principal design criteria can be established to size the tank structure based on loads. For the baseline vehicle in this study, the design criteria include:

1) 22 psi tank ullage pressure.
2) Burst pressure of two times operating pressure.
3) Safety factor of 1.5 on other loads.
4) Design life of 1000 cycles with a scatter factor of 4.
5) 350°F maximum operating temperature for aluminum.
6) 800°F maximum operating temperature for stainless steel.
7) 175°F maximum operating temperature for polyurethane cryogenic foam.
8) 400°F maximum operating temperature for polymethacrylimide cryogenic foam.
9) 32°F temperature on the exterior tank surface to preclude ice/frost formation.
10) Leak-free containment.
11) 0.020 in. minimum gage for aluminum.
12) 0.010 in. minimum gage for stainless steel.

In the parametric studies, the effect of the design g loading and variations in design criteria were evaluated from the criteria listed above.

Materials

The cryogenic propellants, LOX and LH_2, at temperatures of −297 and −423°F, respectively, must be contained by compatible materials. The choice of materials is critical since many materials are LOX-sensitive,[4] and/or embrittled by hydrogen.[5] The low-temperature environment may also reduce ductility and fracture toughness of the tank materials to unacceptably low levels. The structural design criterion of 1000 leak-free cycles required that no cracks grow through the thickness on the tank structures between inspections or for the life of the tank. In cryogenic tanks, a crack through the thickness—while not of a critical size structurally—can be catastrophic because leaking propellants are a fire/explosion hazard. Therefore, for reusable cryogenic tanks, the minimum tank wall thickness must be thicker (10% in this study) than the depth of the largest undetectable crack, which is assumed to be the initial flaw depth. Both 2219 aluminum and AISI 301 stainless-steel materials were studied. Both have moderately high-strength, low-notch sensitivity at cryogenic temperatures, excellent compatibility with both propellants, and excellent weldability.

Table 1 summarizes the physical properties of the 2219 aluminum[6-8] and 301 stainless steel[6-10] at cryogenic, room, and maximum service temperatures.

Analytical Procedure

A computerized analytical method was created to evaluate the large matrix of solutions generated by varying the design requirements and tank sizes. Figure 3 is a descriptive flowchart of this program. The tank skin thickness is initially sized to meet the inertial and burst pressure design criteria based on tank diameter and the ultimate tensile strength of the tank material at its working temperature. The tank of this thickness is evaluated next for its ability to endure the required design life using the fracture mechanics technique of Ref. 11. This requires that an initial surface flaw size be assumed. These initial flaws are semicircular in shape, perpendicular to the surface, and have a surface length two times the crack depth. When required, the skin thickness is increased to meet the fracture mechanics determined life, which lowers the operating stress from that determined by internal pressure.

The tank skin thickness, sized for pressure load and fracture life, is evaluated next for buckling resistance. The bending and thrust loads produce compressive loads on the tank wall. Stiffeners are added where required to prevent buckling as an incremental increase in equivalent skin thickness $\bar{t}$. For a given tank size and wall construction, the added stiffener $\bar{t}$ is primarily a function of the elastic modulus of the tank material unless the compressive load intensity is very high, where the strain limit of the material will determine the tank wall thickness. The tank ullage pressure, when maintained through the flight, imposes an axial tension load in the tank wall which reduces the compressive load generated from the

Table 1 Physical properties of candidate cryogenic tank materials

Property \ Material	2219-T87 Aluminum			Type 301-EH Stainless steel		
	Mechanical properties					
Temperature, °F	−400	RT[a]	300	−400	RT	800
Tension ultimate, ksi	91.0	63.0	48.0	330.0	210.0	170.0
Tension yield, ksi	65.0	51.0	38.0	260.0	190.0	140.0
Compression yield, ksi	65.0	52.0	38.0	260.0	230.0	140.0
Elastic modulus, $\times 10^{-6}$	12.5	10.5	9.5	36.0	26.0	22.1
K_{IC}, *ksi* $\sqrt{\text{in.}}$	78	64	—	180	205	—
Density, lb/in.^{2}		0.102			0.286	
Elongation, %	15.0	10.0	15.0	3.0	9.0	6.0
COE,[b] in./in. °F, $\times 10^6$	8.3	12.3	13.0	5.5	8.6	10.2
Poisson's ratio		0.33			0.33	
C, Btu/lb °F	0.015	0.205	0.220	0.050	0.100	0.135
K, Btu/h-ft^2 °F/ft	14.0	72.0	80.0	2.5	9.0	12.0

[a]RT = room temperature. [b]Coefficient of thermal expansion.

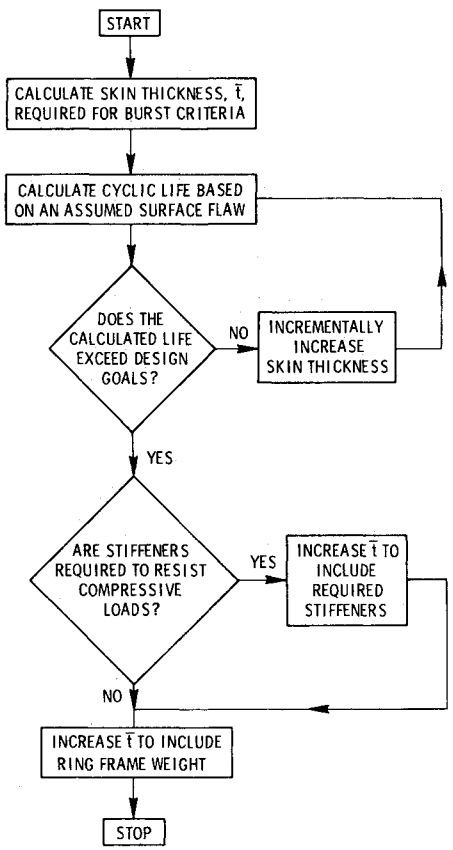

Fig. 3 Structural sizing routine.

bending loads. When the pressure-induced N_x exceeds the compressive bending N_x, or reduces the compressive N_x to a value when no stiffeners are required to resist buckling due to the compressive load, a pressure-stabilized unstiffened skin structure is able to support the loads. Ring frames are then added to the skin, completing the structural design cycle for a tank based on pressure, fracture mechanics, and bending criteria. However, consideration of thermal loads is also required.

Thermal stresses may impact the design of the tank wall, especially for the honeycomb concept when the inner facesheet is at a cryogenic temperature and the outer face is at some temperature greater than 32°F. The temperature difference produces tensile loads on the inner surface and compressive loads on the outer surface as the cold inner surface is restrained from contracting by the warmer outer surface. The increased tensile stresses in the skin must be considered in the pressure and fracture mechanics analyses. Similarly, a nonlinear thermal gradient from the top to the bottom may occur in a partially filled tank because the portion of the tank in contact with the cryogen is colder than the top of the tank. This temperature gradient causes thermal stresses even for a simply supported tank. In the baseline example, a linear thermal gradient is assumed and the simple supports allow the tank to bow, thereby alleviating thermal stresses that can result from a nonlinear thermal gradient or rigid tank supports. In the baseline example, the tank supports were positioned to minimize both the deflection (thermal and bending) and the maximum bending moment simultaneously.

Aeroinertial Loads

The flight trajectories shown in Fig. 4 are typical for the baseline, vertically launched, two-stage, rocket-propelled space transportation system.[12] These trajectories are used to establish the design loads for the baseline cryogenic tank. Figure 5 shows the axial and normal accelerations produced from the ascent trajectory of Fig. 4. The maximum structural loading on the tank occurs just prior to booster staging when an axial acceleration of 2.2g and a normal acceleration of 0.5g are encountered simultaneously with fully fueled tanks. During entry these tanks experience a higher normal acceleration, 2.5g, but are assumed to be empty, thus producing very low loads on the tanks. However, for horizontally launched space vehicles (or for aircraft), the 2.5 g normal loading would occur on the fully fueled tank producing a much higher tank bending load. Also, the ascent and entry trajectories imposed thermal loads on the tank. The effects of the temperature variations on cryogenic tanks are discussed in a later section.

Tank Wall Sizing

The cryogenic tank structure must be sized to resist the loads imposed by the various design criteria. Ullage pressure, aeroinertially induced hydrostatic pressure, and bending loads are considered in sizing a tank wall structure that will meet the tank design life, which is determined by fracture mechanics considerations. The following sections present the analytical procedure and the interaction between the design criteria.

Pressure Loads

Cryogenic propellant tanks must be pressurized above the ambient pressure at which the saturated cryogenic liquids are stored prior to filling the tank in order to minimize boiling of the cryogenic fluids. This internal pressure combined with any additional aeroinertial produced hydrostatic pressure is used to initially size the tank structure.

For example, an ullage pressure of 22 psi on a 30 ft diameter tank (180 in. radius) results in a load of 3960 lb/in. For aluminum with a working stress limit of 22 ksi, a skin

thickness based on hoop tension, $S=PR/t$, of 0.18 in. is required. However, a 301 stainless steel tank wall with a 100-ksi working stress limit requires a skin thickness of 0.04 in. Thus, a stainless-steel tank sized on pressure only using this material allowable would be lighter than an aluminum tank

The hydrostatic head of the propellants can significantly increase the tank wall thickness requirement. A 120 ft long LH_2 tank when standing vertically has a hydrostatic pressure of 3.7 psi at the base, and the 25 ft long LOX tank has a hydrostatic pressure of 12.3 psi at its base due to the higher LOX density. An axial acceleration of $3g$ on the above hydrostatic pressures increases the pressure load at the bottom of the tank by 2000 and 6640 lb/in., respectively, in the hoop direction and by 1000 and 3320/lb/in., respectively, in the axial direction. Therefore, the tank wall thickness was calculated at the top and bottom of the tank to determine the average tank wall thickness required to resist the pressure loads.

Fracture Mechanics

Cycle life is also a design consideration which is highly dependent on material, temperature, stress level, wall thickness, and initial flaw size. Figures 6 and 7 are fracture mechanics curves for 2219-T87 aluminum alloy and AISI 301 stainless steel, respectively. They are derived using crack growth data for the aluminum[13] and stainless steel[14] as input to the computer program based on the method of Ref. 11. An initial flaw depth of 0.05 in. having a surface crack length of 0.10 in. is recommended as the smallest readily detectable flaw size.[15] Figure 6 shows that a minimum thickness of 0.15 in. is required for 2219-T87 aluminum to endure 4000 cycles (1000 cycles with a scatter factor of 4), assuming the 0.050-in. initial flaw depth and an allowable working stress of 29,300 psi. If a smaller flaw were assumed, the tank would have a longer life or a thinner wall thickness for the same life.

The 0.05 in. initial flaw depth assumption requires a stainless-steel tank wall thickness of only 0.08 in. at a working stress level of 100 ksi, as shown in Fig. 7, because stainless steel has better fracture mechanics properties than aluminum. Were a 0.02 in. deep initial flaw assumed in the stainless steel, then a 0.04 in. wall thickness could be used to meet the 4000 cycle life goal at the 100 ksi stress level. As previously indicated, a 180 in. radius tank designed for a 22 psi working pressure load requires that $\bar{t}=0.04$ in. for 100 ksi stainless-steel material. The 0.05 in. flaw assumption would double this tank wall thickness if the 100 ksi stress level were maintained. However, as the tank wall thickness is increased, the stress level is lowered for the same design pressure. The optimum wall thickness is determined to be 0.058 in. by iterative solutions, or an increase in $\bar{t}$ of 45% to satisfy this cycle life criteria. From Fig. 7, a 0.025 in. initial flaw is the largest flaw that would pose no fracture mechanics penalty on the stainless steel tank concept.

Bending Loads

The tank-thrust structure is supported on aft-located trunnions and forward-located hinged supports (Fig. 1) to allow for thermal growth between the airframe and tank. Since a large section of this tank is cantilevered in front of the forward hinged support, the bending moments produced by normal accelerations are much higher than those for a more conventional, simply supported tank system. The bending moments for the baseline, fully loaded, Orbiter tanks are shown in Fig. 8 for 2.5 and 0.5 g normal accelerations which are representative of horizontal and vertical launch vehicles, respectively,

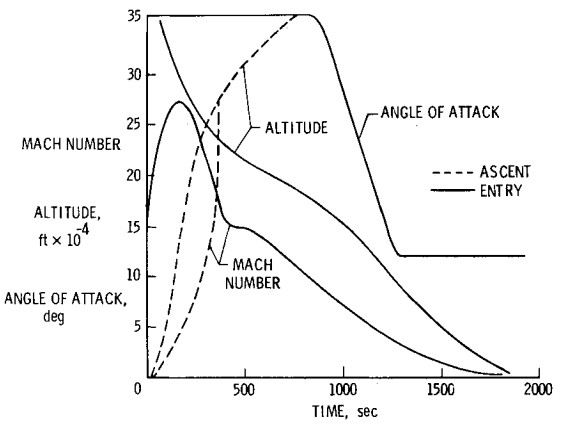

Fig. 4 Typical ascent and entry trajectories for space launch vehicles.

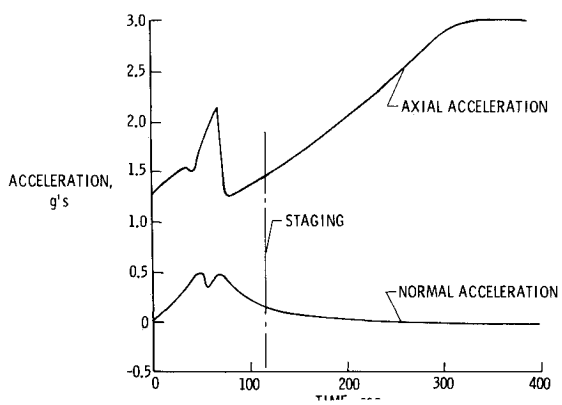

Fig. 5 Ascent accelerations for vertically launched two-stage baseline vehicle.

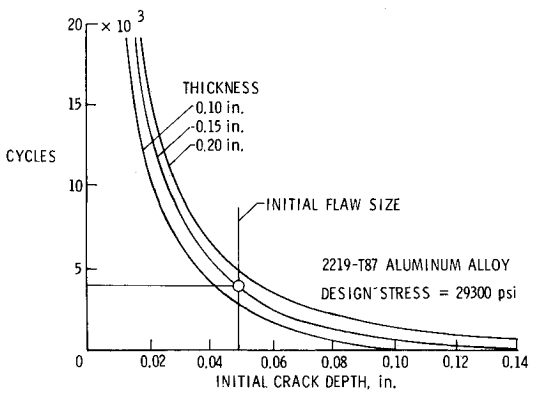

Fig. 6 Fracture mechanics considerations for 2219-T87 aluminum alloy.

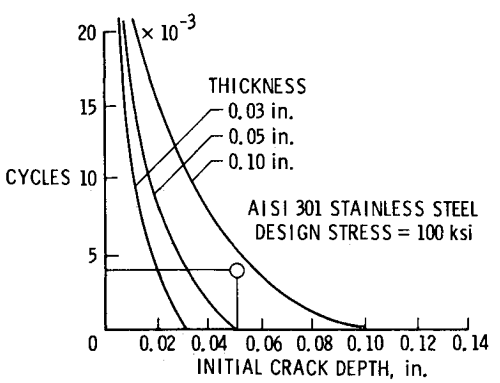

Fig. 7 Fracture mechanics considerations for AISI 301 stainless steel.

for these fully loaded, 30 ft diam tanks. Using a weight-strength curve, such as Fig. 9 or 10, the wall thickness t required for a given wall construction can be determined for both the strain-limited and buckling-critical portions of the tank.

Figures 9 and 10 are weight-strength curves for aluminum and stainless steel, respectively, which show the weight index $\bar{t}/R$ as a function of the load index N/RE. They are bounded by the material strain limit and the least thickness unstiffened skin required to support the compressive load. The 0.3 and 0.4% strain limits are consistent with the working stress levels and the design cycle life requirements.[16] Optimum curves for both honeycomb-core sandwich and integrally stiffened skin cylinder walls from Ref. 17 are indicated. These optimum values are based on buckling resistance and have no constraints for minimum gage or other design requirements.

The $\bar{t}/R$ values for reusable cryogenic tank applications are shown to be much higher than the optimum $\bar{t}/R$ values. These curves are based on the previously related requirements—1000 cycle lifetime, a 0.05-in. initial flaw, and 22-psi working pressure—which establish a minimum thickness for the tank wall based on its diameter. These curves are shown for a 180 in. radius tank for an integrally stiffened tank wall and a honeycomb-core sandwich tank wall for aluminum in Fig. 9 and stainless steel in Fig. 10. The range of load index for the 180 in. radius baseline tank is also indicated on these figures for the 0.5 and 2.5 g load cases. The honeycomb tank wall is thicker than required for an optimum core, because the core depth is sized to provide the cryogenic insulation and, therefore, is capable of withstanding the bending loads with no weight increase. The thermal design requirements for the core will be discussed in a later section.

The integrally stiffened skin curve for aluminum indicates that some stiffeners are required on the tank wall when the load index is between 3×10^{-7} and 3×10^{-5}. Below a load index of 3×10^{-7}, an unstiffened skin thickness based on pressure alone is thicker than required to resist buckling. Also, the tension load from the 22 psi ullage pressure is higher than the maximum compressive load from bending. Therefore, when tank pressurization is maintained, the tank skin is always in tension and no stiffeners are required for the 0.5 g load. As shown, the 2.5 g load produces a compressive load intensity that requires a pressure greater than 22 psi to maintain tension in the tank skin. Therefore, for the 2.5 g load, some stiffeners will be required. The $\bar{t}$ required to resist the bending-induced loads for cylindrical tanks of different diameters and for both aluminum and stainless-steel materials can be calculated in this manner.

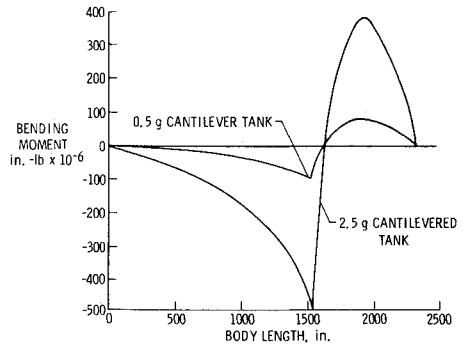

Fig. 8 Tank bending moments for simply supported and cantilever tank supports.

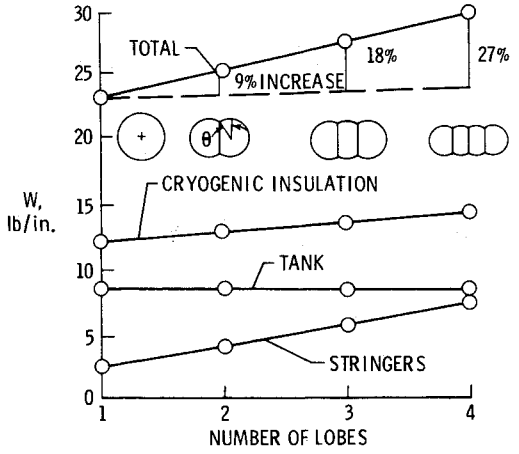

Fig. 9 Structural index curves of optimized cylinders, aluminum.

Multilobe Tanks

Propellant tanks are normally required to be volumetrically efficient and, therefore, to conform to the shape of a vehicle that may not have a circular cylinder cross section due to aerodynamic considerations. Noncircular cross-section tanks are not as structurally efficient as circular cross-section cylindrical tanks[18] and were not considered in this study. However, better volumetric efficiency within a given cross section may be required than is available from a single circular section tank. Therefore, an analysis of tank weight was made for optimized intersecting circular cylinders forming multilobe or pillow tanks. The results of this analysis for a constant cross-sectional area of 707 ft^2 (30-ft-diam cylinder) are presented in Fig. 11. The $\bar{t}$ required to resist bending loads will increase as N_x increases, resulting from the tank height decrease with an increasing number of lobes. Also, since there is more surface area on a multilobe tank, more insulation is required. The structural weight of the tank skin remains nearly constant. The skin thickness decreases due to the smaller diameter, but the circumference is greater an an internal web is required to resist the load at the lobe intersection.

The intersection angle θ (Fig. 11) for a multilobe tank design is determined first. For single skin aluminum tank wall con-

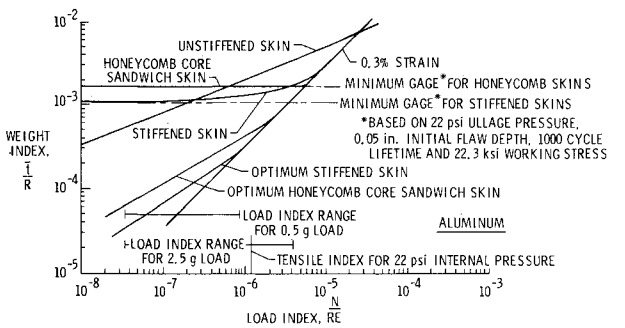

Fig. 10 Structural index curves of optimized cylinders, stainless steel.

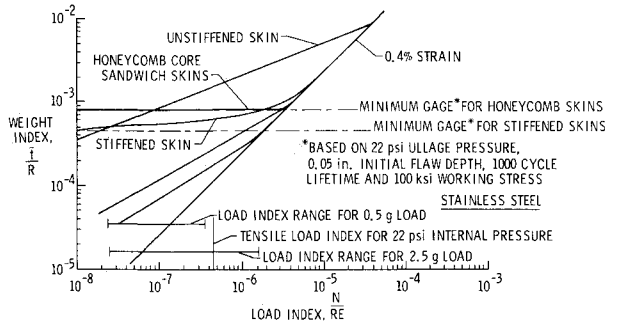

Fig. 11 Tank weight variation with the number of lobes for a 707 ft^2 area.

struction, the weight penalty based on pressure sizing increases from a single circular cylinder ($\theta = 0$ deg) to a maximum of 5% at $\theta = 45$ deg. A design incorporating two separate circular cylinders ($\theta = 90$ deg) also has no pressure-induced weight penalty. This modest pressure sizing weight penalty is due to a combination of reduced volumetric efficiency and the inclusion of a web (connecting the opposite sections of the cylindrical lobes). The web thicknesses are sized such that the web radial displacement satisfies the zero hoop bending stress condition.

If insulation requirements are not a large part of the wall weight, and tank bending moments are low so that stiffening is not a significant weight driver, then all angles of θ are feasible. Pressure stabilization and increased insulation system efficiency reduce the penalty for multicylinder designs.

When skin thicknesses are constrained by fracture mechanics criteria or minimum gage, the penalty for a multilobe tank design is much greater. $\bar{t}$ increases because a web is added, and simultaneously the volumetric efficiency diminishes. For the baseline tank design conditions used in this study, weight penalties are large at all θ values, e.g., 30% at $\theta = 5$ deg, and, in the limit of a two-cylinder design, a 40% weight penalty occurs.

For a given enclosed area, as θ increases skin gages will decrease to maintain the design stress. With decreasing skin gages, fracture mechanics limits the minimum wall thicknesses. This penalty is similar to the minimum gage constraint, however, when 0.05-in.-deep flaws are assumed, the minimum thickness is greater than 0.05 in. Initial flaw size assumptions constrain the external tank wall thicknesses, but because through-the-thickness cracks are allowable in the web the web gages will be affected less by fracture mechanics considerations.

Honeycomb-core sandwich multilobe tanks are affected more by the minimum gage and fracture mechanics limitations than a single skin tank design because thinner sheet gages are required for strength. When honeycomb core weight is greater than the weight required for a foam insulation, that weight difference is compounded by multilobe volumetric inefficiency because the insulation system weight is a function of surface area. Complex nonoptimum joint designs are also incurred with a multilobe honeycomb construction since thermal stresses as well as pressurization stresses are involved in the web-cylinder displacement solution.

Thermal Analysis

Each tank design concept requires cryogenic insulation, as shown in Fig. 2, to prevent air liquefaction and frost or ice buildup during ascent, Also, aerodynamic heating of the fuselage, especially during atmospheric entry, will require a thermal protection system (TPS) to insulate the tank or its cryogenic insulation from these high temperatures and keep the tank structure and cryogenic insulation below their maximum operating temperature. To evaluate the insulation and TPS requirements for the baseline vehicle, which has a hot fuselage structure, the trajectories of Fig. 4 were used as input to a two-dimensional transient heating code.[19]

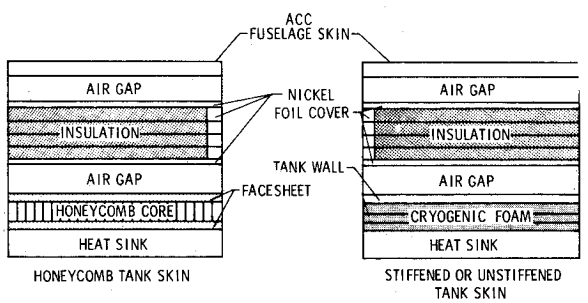

Fig. 12 Thermal models of cryogenic tank wall concepts.

Two cryogenic foam systems were evaluated. The first, a polyurethane foam, is similar to the Saturn S-IV-B insulation with a 175°F temperature limit for reusability. The second foam is a more advanced polymethacrylimide foam that may have a reuse temperature of 400°F.

The tank structural concepts and insulation systems were simulated with thermal models similar to those shown in Fig. 12. Both models have a hot fuselage containing packaged internal fibrous insulation for the TPS. An integrally stiffened tank with internal cryogenic foam is shown on the left-hand side, and a honeycomb tank is shown on the right in Fig. 12. The two-dimensional transient heating analysis calculates the temperature history of each element of the model.

For this study, two axial locations were used to determine TPS and insulation requirements on the upper and lower surfaces of the baseline vehicles. Points 100 and 1800 in. aft of the nose were used for the hydrogen and oxygen tanks, respectively.

The thicknesses of the cryogenic foam (both internal and external) and the honeycomb core were determined for this application. These are the minimum insulation thicknesses to maintain the surface of the tank above 32°F during the ascent portion of the launch of the baseline space transportation system. These foam and core thicknesses are shown in Tables 2 and 3 for several concepts for LH_2 and LOX tank walls, respectively. During the ground hold time, a dry, warm air purge system is used to prevent frost or ice formation; otherwise, an unacceptably thick foam insulation would be required.

A typical thermal history during entry for the baseline vehicle with an aluminum skin and internal cryogenic foam insulation (limited to 175°F) is shown in Fig. 13. The thickness of the packaged fibrous insulation TPS was varied until that thickness required to maintain the foam below the 175°F temperature limit was determined. The TPS thicknesses were determined for the upper and lower surfaces of several LH_2 and LOX tank concepts and are presented in Tables 2 and 3, respectively.

The average TPS and insulation thicknesses are established by having 25% of the tank circumference covered with the lower surface thicknesses and the remainder of the tank covered with the upper surface thicknesses. The total TPS and insulation volume is then divided by the tank area to establish the average requirements.

A cryogenic hydrogen tank may have the foam on the inner or outer tank surface. On the inner surface the foam will be permeated by hydrogen gas, which increases the conductivity of the foam, requiring more foam. However the aluminum material on the outer surface is a very good heat sink. When the foam is on the outer surface of the tank it has a low conductivity, but its outer surface is limited to 175°F and the outer surface of the foam has no heat sink to prevent its temperature from rising. The analysis indicates that the ex-

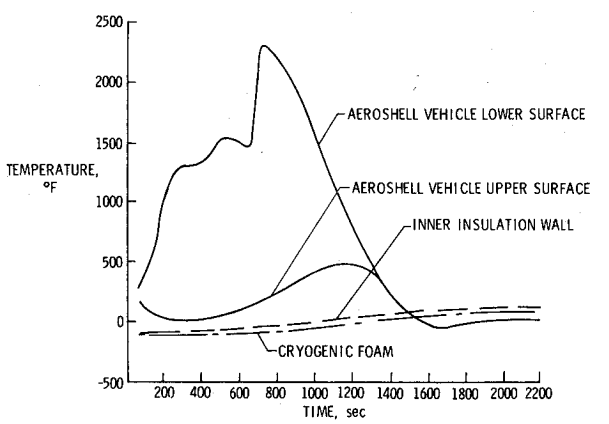

Fig. 13 Entry thermal history for a space vehicle with an internally insulated aluminum tank.

Table 2 Summary of LH_2 tank insulation thickness requirements, in.

	Cryogenic foam insulation					Honeycomb insulation	
	Aluminum			Stainless steel, interior		Facesheets, 1% titanium core	
Tank concept	Int. 175°F	Ext. 175°F	Int. 400°F	175°F	400°F	Aluminum	Stainless steel
Lower surface:							
Air gap	0.25	0.25	0.25	0.25	0.25	0.25	0.25
Fibrous insulation	3.9	6.7	2.1	4.5	2.2	1.7	0.52
Air gap	3.0	3.0	3.0	3.0	3.0	3.0	3.0
Foam	0.4	3.5	0.4	0.6	0.6	—	—
Core	—	—	—	—	—	0.33	0.55
Upper surface:							
Air gap	0.25	0.25	0.25	0.25	0.25	0.25	0.25
Fibrous insulation	0.0	0.0	0.0	0.0	0.0	0.0	0.0
Air gap	3.0	3.0	3.0	3.0	3.0	3.0	3.0
Foam	0.4	3.5	0.4	0.6	0.6	—	—
Core	—	—	—	—	—	0.33	0.55
Averages:							
Fibrous insulation	1.0	2.6	0.5	1.1	0.6	0.4	0.1
Foam/core	0.4	3.5	0.4	0.6	0.6	0.33	0.55

Table 3 Summary of LOX tank insulation thickness requirements, in.

	Cryogenic foam insulation				Honeycomb insulation	
	Aluminum, exterior		Stainless steel, exterior		Facesheets, 1% titanium core	
Tank concept	175°F	400°F	175°F	400°F	Aluminum	Stainless steel
Lower surface:						
Air gap	0.25	0.25	0.25	0.25	0.25	0.25
Fibrous insulation	5.8	3.0	5.8	3.0	0.9	0.1
Air gap	3.0	3.0	3.0	3.0	3.0	3.0
Foam	2.5	2.5	2.5	2.5	—	—
Core	—	—	—	—	0.30	0.45
Upper surface:						
Air gap	0.25	0.25	0.25	0.25	0.25	0.25
Fibrous insulation	0.0	0.0	0.0	0.0	0.0	0.0
Air gap	3.0	3.0	3.0	3.0	3.0	3.0
Foam	2.5	2.5	2.5	2.5	—	—
Core	—	—	—	—	0.30	0.45
Averages:						
Fibrous insulation	1.5	0.8	1.5	0.8	0.2	0.03
Foam/core	2.5	2.5	2.5	2.5	0.30	0.45

terior 175°F foam system requires four times the total insulation thickness (the sum of the fibrous insulation TPS and cryogenic foam) for a LH_2 tank than for an internally mounted foam system, as shown in Table 2. a 400°F temperature limit cryogenic foam requires one-half the thickness of the lower surface TPS that a 175°F foam requires while having a minimal effect on the upper surface TPS. This internal 400°F-limit foam has the minimum total insulation thickness for single wall LH_2 tanks. However, as shown in Tables 2 and 3, the honeycomb concepts require less total thickness to provide the required insulation, and the core density, 1%, is lower than the cryogenic foam density.

Weights

The unit weight of the structural elements and required insulation and TPS were calculated for the baseline vehicle using the analytical procedures previously described. Tables 4 and 5 compare the unit weights of several wall constructions for LH_2 and LOX tanks, respectively. As indicated, the unstiffened skin aluminum tank (pressure stabilized) with cryogenic insulation capable of a 400°F reuse temperature is the least weight for both the LH_2 and LOX tanks for the baseline vehicle. The 400°F reuse temperature foam reduces the total cryogenic insulation and TPS weight by up to 50% when compared with a 175°F reuse temperature foam. The foam and TPS comprise between 10 and 36% of the tank wall weight for the cryogenic-foam-insulated concepts. The honeycomb-core sandwich tank concepts have lower insulation (core) and TPS weights; however, due to the thicker facesheets required to meet the fracture mechanics criteria, the lightest honeycomb tanks are 20-40% heavier than the lightest foam-insulated tanks.

Table 4 Summary of unit weights for LH_2 tank concepts, psf

Tank wall construction	Unstiffened skin: Aluminum foam Int. 175°F	Ext. 175°F	Int. 400°F	Ext. 400°F	Stainless steel foam Int. 400°	Ext. 400°	Stiffened skin: Aluminum foam Int. 175°F	Ext. 175°F	Int. 400°F	Ext. 400°F	Stainless steel foam Int. 400°F	Ext. 400°F	Honeycomb skin titanium core: Aluminum facesheets	Stainless steel facesheets
Lower surface:														
Aeroshell	1.00	1.00	1.00	1.00	1.00	1.00	1.00	1.00	1.00	1.00	1.00	1.00	1.00	1.00
Fibrous insulation	1.10	1.90	0.60	1.20	0.63	1.30	1.10	1.90	0.60	1.20	0.63	1.30	0.49	0.15
Foil package	0.68	0.88	0.56	0.69	0.56	0.73	0.68	0.88	0.56	0.69	0.56	0.73	0.53	0.45
Foam	0.08	0.73	0.10	0.90	0.15	0.13	0.08	0.73	0.10	0.90	0.15	0.13	—	—
Honeycomb core	—	—	—	—	—	—	—	—	—	—	—	—	0.08	0.13
Tank	2.80	2.80	2.80	2.80	3.40	3.40	3.00	3.00	3.00	3.00	3.90	3.90	4.52	5.80
Upper surface:														
Aeroshell	1.00	1.00	1.00	1.00	1.00	1.00	1.00	1.00	1.00	1.00	1.00	1.00	1.00	1.00
Fibrous insulation	0.00	0.35	0.00	0.00	0.00	0.00	0.00	0.35	0.00	0.00	0.00	0.00	0.00	0.00
Foil package	0.00	0.49	0.00	0.00	0.00	0.00	0.00	0.49	0.00	0.00	0.00	0.00	0.00	0.00
Foam	0.08	0.73	0.10	0.90	0.15	0.13	0.08	0.73	0.10	0.90	0.15	0.13	—	—
Honeycomb core	—	—	—	—	—	—	—	—	—	—	—	—	0.08	0.13
Tank	2.80	2.80	2.80	2.80	3.40	3.40	2.80	2.80	2.80	2.80	3.40	3.40	4.52	5.80
Averages:														
Aeroshell	1.00	1.00	1.00	1.00	1.00	1.00	1.00	1.00	1.00	1.00	1.00	1.00	1.00	1.00
Fibrous insulation	0.28	0.84	0.15	0.30	0.16	0.33	0.28	0.84	0.15	0.30	0.16	0.33	0.12	0.04
Foil package	0.17	0.59	0.15	0.20	0.14	0.18	0.17	0.59	0.15	0.20	0.14	0.18	0.13	0.11
Foam	0.08	0.73	0.10	0.90	0.15	0.13	0.08	0.73	0.10	0.90	0.15	0.13	—	—
Honeycomb core	—	—	—	—	—	—	—	—	—	—	—	—	0.08	0.13
Tank	2.80	2.80	2.80	2.80	3.40	3.40	2.90	2.90	2.90	2.90	3.5	3.5	4.52	5.80
Total	4.33	5.96	4.20	5.20	4.85	5.04	4.43	6.06	4.30	5.30	4.95	5.14	5.85	7.08

Table 5 Summary of unit weights for LOX tank concepts, psf

Tank wall construction	Unstiffened skin: Aluminum exterior foam 175°F	400°F	Stainless steel exterior foam 175°F	400°F	Stiffened skin: Aluminum exterior foam 175°F	400°F	Stainless exterior foam 175°F	400°F	Honeycomb skin titanium core: Aluminum facesheets	Stainless steel facesheets
Lower surface:										
Aeroshell	1.00	1.00	1.00	1.00	1.00	1.00	1.00	1.00	1.00	1.00
Fibrous insulation	1.70	0.86	1.70	0.86	1.70	0.86	1.70	0.86	0.26	0.03
Foil package	0.82	0.62	0.82	0.62	0.82	0.62	0.82	0.62	0.47	0.42
Foam	0.52	0.65	0.52	0.65	0.52	0.65	0.52	0.65	—	—
Honeycomb core	—	—	—	—	—	—	—	—	0.07	0.11
Tank	2.80	2.80	3.40	3.40	2.80	2.80	3.40	3.40	4.52	5.80
Upper surface:										
Aeroshell	1.00	1.00	1.00	1.00	1.00	1.00	1.00	1.00	1.00	1.00
Fibrous insulation	0.00	0.00	0.00	0.00	0.00	0.00	0.00	0.00	0.00	0.00
Foil package	0.20[a]	0.00	0.00	0.00	0.20[a]	0.00	0.00	0.00	0.00	0.00
Foam	0.52	0.65	0.52	0.65	0.52	0.65	0.52	0.65	—	—
Honeycomb core	—	—	—	—	—	—	—	—	0.07	0.11
Tank	2.80	2.80	3.40	3.40	3.10	3.10	3.90	3.90	4.52	5.80
Averages:										
Aeroshell	1.00	1.00	1.00	1.00	1.00	1.00	1.00	1.00	1.00	1.00
Fibrous insulation	0.43	0.22	0.43	0.22	0.43	0.22	0.43	0.22	0.07	0.01
Foil package	0.36	0.16	0.21	0.16	0.36	0.16	0.21	0.16	0.12	0.11
Foam	0.52	0.65	0.52	0.65	0.52	0.65	0.52	0.65	—	—
Honeycomb core	—	—	—	—	—	—	—	—	0.07	0.11
Tank	2.80	2.80	3.40	3.40	2.90	2.90	3.50	3.50	4.52	5.80
Total	5.11	4.83	5.56	5.43	5.21	4.93	5.60	5.53	5.78	7.03

[a] Radiation barrier.

Conclusions

Thermostructural analyses of reusable flight-weight cryogenic tanks for a vertically launched space vehicle were conducted. An analytical procedure was developed for sizing the tank structure, cryogenic insulation, and thermal protection system. Unstiffened, integrally stiffened, and honeycomb-core sandwich tank skins using aluminum or stainless steel materials were compared for their ability to meet design criteria at least weight. Cryogenic insulation systems were also evaluated including closed-cell cryogenic foams and an evacuated honeycomb core. The results indicate that a 400°F foam insulated, unstiffened-skin aluminum tank structure is the lightest structure for either LOX or LH_2 tanks that meets the selected design criteria, but only 2-4% lighter than a stiffened aluminum tank. A cryogenic foam insulation with a 400°F reuse temperature is shown to save up to 50% of the total thermal protection system and insulation weight compared with a 175°F reuse temperature foam. A reusable tank structure is primarily sized by pressure and fracture mechanics criteria, while the aeroinertially induced bending loads do not affect tank weight significantly. The results indicate that the development of 400°F reuse temperature foam and the development of procedures for the reliable detection of small material flaws, less than 0.05 in. deep, show promise for reducing the cyrogenic tank weight by up to 50%.

References

[1]Lessaro, R. E., "Liquid Hydrogen as a Fuel for Future Commercial Aircraft," *Hydrogen Energy*, Pt. B, Plenum Press, 1974, pp. 839-857.

[2]Taylor, A. H., Jackson, L. R., MacConachie, I. O., and Martin, J. A., "The FSTS Study—Structures and Subsystems," *Astronautics & Aeronautics*, Vol. 21, June 1983, pp. 50-62.

[3]Taylor, A. H., Jackson, L. R., Davis, R., Cerro, J. A., and Scotti, S. J., "Structural Concepts for Future Space Transportation System Orbiters," *Journal of Spacecraft and Rockets*, Vol. 22, May-June 1985, pp. 333-339.

[4]White, E. L. and Ward, J. J., "Ignition of Metals in Oxygen," Defense Metals Information Center Battelle Memorial Institute, Columbus, OHio, Rept. 224, Feb. 1966.

[5]Chandler, W. T., "Hydrogen Embrittlement and Its Control in Hydrogen Fueled Engine Systems," NASA CP 2065, Pt. I, Sept. 1978, pp. 195-252.

[6]Brewer, G. P. et al., "Study of Fuel Systems for LH_2 Fueled Subsonic Transonic Aircraft," NASA CR 145369, July 1978.

[7]*Military Standardization Handbook—Metallic Materials and Elements for Aerospace Vehicle Structures*, MIL-HDBK-5C, Sept. 1976.

[8]U.S. Department of Defense, *Aerospace Structural Metals Handbook*, Dec. 1978.

[9]Witzell, W. E., "Fracture Toughness of Stainless Steel Sheet at Cryogenic Temperatures," ARS Paper 2418-62, April 1962.

[10]Calfo, F. E., "Cryogenic Fracture Properties of Thin AISI 301 60 Percent Cold Reduced Sheet at Various Angles to the Rolling Direction," NASA TN D 5413, Sept. 1969.

[11]Newman, J. C. and Raju, I. S., "Analysis of Surface Cracks in Finite Plates Under Tension and Bending Loads," NASA TP 1578, Dec. 1979.

[12]Taylor, A. H., Jackson, L. R., Davis, R., Cerro, J. A., and Scotti, S. J., "Structural Concepts for Future Space Transportation System Orbiters," AIAA Paper 83-0210, Jan. 1983.

[13]Witzell, W. E., "Evaluation of Mechanical Property Data on the 2219 Aluminum Alloy and Application of the Data to the Design of Liquid Hydrogen Tankage," NASA CR 145140, 1977.

[14]Pineau, A. G. and Pelloux, R. M., "Influence of Strain Induced Martensitic Transformations on Fatigue Crack Growth Rates in Stainless Steel," *Metallurgical Transactions*, Vol. 5, May 1974, pp. 1103-1112.

[15]"Military Standard, Aircraft Structural Integrity Program, Airplane Requirements," MIL-STD-1530 (USAF), Sept. 1972.

[16]Simons, H., Rhodes, J. E., and James, A. M., "Strain Barrier Ultimate Cut-Off for Aircraft Structures," presented at the Third *International Conference on Composite Materials*, Paris, France, Aug. 1980.

[17]Shideler, J. L., Anderson, M. S., and Jackson, L. R., "Optimum Mass-Strength Analysis for Orthotropic Ring Stiffened Cylinders Under Axial Compression," NASA TN D 6772, 1972.

[18]Shanley, F. R., *Weight Strength Analysis of Aircraft Structures*, 2nd Ed., Dover Publications, New York, 1960, pp. 215-260.

[19]Garrett, B. and Pitts, J. I., "A General Transient Heat-Transfer Computer Program for Thermally Thick Walls," NASA TM X 2058, Aug. 1970.